

# LeNEPA: No-Augmentation Next-Latent Prediction for Time-Series Representation Learning

Alexander Chemeris  
Langotime  
South Africa  
alex@langotime.ai

Ming Jin  
Griffith University  
Australia

Randall Balestriero  
Brown University  
United States

## Abstract

Time series are central to modern data mining applications, from industrial telemetry and server metrics to finance and physiology, yet time-series self-supervised learning often depends on view and augmentation choices that encode domain-specific invariances. We study a narrower practical question than fully tuned benchmark performance: how does an SSL recipe behave when its method-specific configuration is reused unchanged after the pretraining signal family changes? We frame this as a fixed-recipe stress test rather than as a comparison against optimally tuned methods. We introduce Latent Euclidean Next-Embedding Prediction Architecture (LeNEPA), a no-augmentation next-latent-token prediction objective with a causal backbone. LeNEPA replaces the stop-gradient/EMA stabilization used by vanilla NEPA with SIGReg-based isotropy regularization and computes the predictive loss in a lightweight projected space that is discarded for evaluation. We compare LeNEPA with an ECG-tuned JEPA recipe under a fixed-horizon frozen-probe protocol on PTB-XL and Diag, a synthetic diagnostic corpus generated with Aionoscope. Both methods are retrained independently on each dataset, but their method-specific recipes are kept unchanged: LeNEPA keeps the same no-augmentation objective configuration, while JEPA keeps the same ECG-tuned masking recipe. In this protocol, the ECG-tuned JEPA recipe is strong in-domain on PTB-XL but weaker when reused unchanged on Diag, whereas LeNEPA preserves useful frozen-probe gains on both datasets. Learning curves suggest faster early representation acquisition under this fixed-horizon protocol: LeNEPA reaches 80% of its final AUROC/AUPRC gain after 2–5k updates, compared with 5–10k updates for the faster JEPA readout. As a separate external frozen-encoder check, a CauKer-pretrained LeNEPA variant reaches 77.65% mean UCR-128 Random-Forest accuracy in a single-seed, best-checkpoint run—within 1.16 points of Mantis and within 0.24 points of MOMENT (77.89%). Overall, the results support no-augmentation latent prediction as a useful candidate recipe for low-retuning time-series SSL. Source code and artifacts are available at <https://github.com/langotime/lenepa-milets-2026>.

## CCS Concepts

• **Computing methodologies** → **Machine learning**; • **Mathematics of computing** → *Time series analysis*.

## Keywords

time-series self-supervised learning, time-series representation learning, joint embedding predictive architectures, augmentation-free learning, frozen-feature time-series encoders

## 1 Introduction

Time series are the natural interface to an evolving world: they record how systems change, spanning server metrics, sensor streams, industrial and telecommunication telemetry, finance, and physiology. As analytical systems and AI agents increasingly monitor, diagnose, and intervene in real time, portable pretraining recipes become useful infrastructure for downstream classification, anomaly understanding, root-cause analysis, and clinical diagnosis support. Despite rapid progress for images and text, however, building time-series encoders that require little per-dataset engineering remains difficult: pipelines are still task-specific, and pretrained backbones are far from standardized. A practical SSL recipe should therefore expose compact sequence embeddings while reducing the amount of view, augmentation, and probe engineering needed for each new data source.

Many successful self-supervised objectives (contrastive learning [7, 15], masked reconstruction [14], and modern JEPA variants [1–3]) rely on carefully designed views that preserve task-specific semantics. In vision, this design space is comparatively well understood, yet representation quality can still be sensitive to view engineering: in DINO, removing multi-crop views reduces ImageNet linear-probe top-1 from 76.1% to 72.5% (ViT-S/16), and varying the multi-crop scale split shifts k-NN top-1 from 65.6% to 69.8% [5]; this dependence is even stronger in SimCLR and BYOL [7, 13]. In time series—where what constitutes a “safe” transformation depends on data type, sampling, and downstream semantics [9, 18, 22, 25]—this sensitivity is amplified: an augmentation study reports that augmentation choice alone can create up to 32 accuracy points on a fault-detection dataset, and that the best augmentation reaches F1 0.6975 vs. 0.4811 with no pretraining [17]. In our experiments, small changes in augmentation recipes for time-series JEPA lead to large swings in representation quality (Section 5).

These considerations expose a trade-off. Augmentation-based JEPA-style methods [1] are well studied and can produce strong representations (e.g., ECG\_JEPA for PTB-XL [21]), but their performance depends critically on augmentation choices. **When a view recipe is reused outside the domain it was designed for, augmentation engineering can become a practical bottleneck for reusable time-series SSL recipes.**

### Contributions.

- We propose LeNEPA, a *no-augmentation next-embedding prediction architecture* for frozen-backbone time-series representation learning, adapting SIGReg and Guillotine Regularization to autoregressive latent prediction to remove stop-gradient/EMA stabilization from the tested recipe.

- We evaluate fixed-recipe pretraining reuse across real ECG data and Diag, a synthetic diagnostic corpus generated with the Aionoscope library [6], separating recipe portability from checkpoint transfer: LeNEPA preserves useful frozen-probe gains when reused unchanged, while an ECG-tuned JEPa view recipe is strong in-domain but weaker when its fixed recipe is reused on a structurally different signal family.
- We compare a frozen CauKer-pretrained LeNEPA encoder on UCR-128 against Mantis, NuTime, and MOMENT Random-Forest protocol anchors, using no handcrafted augmentations.

## 2 LeNEPA – lean no-augmentation SSL architecture

We introduce **Latent Euclidean Next-Embedding Prediction Architecture (LeNEPA)**, a lean no-augmentation Self-Supervised Learning (SSL) architecture based on Next-Embedding Prediction Architecture (NEPA) [24]. We split the input data (univariate or multivariate time series) into a sequence of ViT-style patch embeddings with strided convolution and process the sequence with a causal transformer backbone [19]. LeNEPA learns by autoregressively predicting the next latent token: at each index  $t$ , it predicts a token and minimizes the mean squared error to the target at  $t+1$ .

Vanilla NEPA stabilizes training with a teacher network updated by an exponential moving average (EMA) and by blocking gradients through the targets; LeNEPA replaces this mechanism with **Sketched Isotropic Gaussian Regularization (SIGReg)** [2], which regularizes the token embedding distribution toward an isotropic Gaussian. Following Guillotine Regularization [4], we compute the prediction loss in a projected space and discard the projector at evaluation time. Let  $x \in \mathbb{R}^{B \times C \times L}$ , let  $z = \tau_\theta(x) \in \mathbb{R}^{B \times T \times D}$  be strided-convolution patch embeddings, and let  $\hat{z} = f_\phi(z)$  be causal transformer outputs, where  $\hat{z}_{b,t}$  depends only on  $z_{b,1:t}$ . With projector  $h_\psi : \mathbb{R}^D \rightarrow \mathbb{R}^d$ , the LeNEPA prediction loss is

$$\mathcal{L}_{\text{pred}} = \frac{1}{B(T-1)} \sum_{b=1}^B \sum_{t=1}^{T-1} \|h_\psi(\hat{z}_{b,t}) - h_\psi(z_{b,t+1})\|_2^2. \quad (1)$$

Unlike NEPA, LeNEPA does not stop gradients through the target tokens in Eq. (1); stabilization comes from SIGReg.

For time series, global non-collapse is insufficient because tokens can also collapse along the temporal axis within each sample. Batch-wise or pooled SIGReg can keep an aggregate representation non-degenerate while still allowing collapse over the temporal axis; temporal SIGReg instead regularizes the token set inside each sample, directly counterbalancing the next-token regression pressure. Let  $u^{(\ell)} \in \mathbb{R}^{B \times T \times d}$  denote projected patch-token embeddings from layer  $\ell$ . Unlike SIGReg regularization in the original LeJEPa design, we find that SIGReg over the temporal axis works best as a LeNEPA stabilizer: it regularizes the set of patch tokens within each sample,

$$\mathcal{L}_{\text{SIG}}^{\text{time}} = \frac{1}{B|\mathcal{L}_T|} \sum_{t \in \mathcal{L}_T} \sum_{b=1}^B \text{SIGReg}(\{u_{b,t}^{(\ell)}\}_{t=1}^T). \quad (2)$$

The main objective is

$$\mathcal{L} = \lambda_{\text{pred}} \mathcal{L}_{\text{pred}} + \lambda_T \mathcal{L}_{\text{SIG}}^{\text{time}}, \quad (3)$$

with  $\lambda_T = 20$  and  $\mathcal{L}_T = \{0, 8\}$  in the main PTB-XL/Diag configuration; this setting was selected from ablations run on PTB-XL (Table 5). We also evaluated batch-wise (B), pooled-representation (R), innovation/difference (I), and combined BRI placements; temporal (T) SIGReg was the only single-component placement with sustained frozen-backbone gains across both datasets.

### Listing 1: Compact LeNEPA training step

```
# x: [B, C, L]
z = patch_embed(x) # [B, T, D]
tokens = causal_transformer(z) # list of per-layer [B, T, D]
z_hat = tokens[-1] # top-layer predictions

pred = projector(z_hat[:, :-1])
target = projector(z[:, 1:]) # no stop-gradient in LeNEPA
loss = lambda_pred * mse(pred, target)

u_T = [projector(tokens[l]) for l in sigreg_time_layers]
loss += lambda_T * SIGReg_time_per_sample(u_T)

loss.backward()
optimizer.step()
```

When evaluating frozen backbones, we find that intermediate layers provide stronger representations than the final layer for NEPA and LeNEPA (Section 5; Figure 4). This is expected for next-embedding objectives: upper backbone blocks can partially act as an implicit predictor that maps features into the next-token regression space. Therefore, we probe all backbone layers; headline LeNEPA classification readouts use a fixed mid-layer, while best-layer values are retained for baselines and diagnostic analyses where they should be read as oracle upper bounds.

## 3 Evaluation Protocol

We evaluate representations with frozen-backbone probes because our goal is to test whether a pretraining recipe produces useful sequence embeddings when reused unchanged. Throughout the paper, **LeNEPA** denotes the objective and architecture, not a single shared checkpoint or foundation encoder. We use three separately pretrained LeNEPA encoders: **LeNEPA-PTBXL**, trained on PTB-XL [20]; **LeNEPA-Diag**, trained on Diag, a synthetic time-series corpus generated with Aionoscope [6]; and **LeNEPA-CauKer**, trained on CauKer [23]. These checkpoints share the same no-augmentation latent-prediction recipe, but their weights are trained independently.

We separate two evaluation questions to avoid conflating recipe reuse with checkpoint transfer. **Fixed-recipe pretraining reuse** asks whether the same SSL objective configuration can be reused when the pretraining distribution changes, without re-designing method-specific augmentations or loss hyperparameters. We test this by training both methods independently on both datasets: LeNEPA-PTBXL and LeNEPA-Diag use exactly the same no-augmentation objective configuration, while JEPa-PTBXL and JEPa-Diag use the same ECG-tuned view recipe. In both cases, only the pretraining dataset changes. Crucially, both recipes were developed and fixed using PTB-XL experiments: the JEPa masking schedule was tuned for ECG morphology, and the LeNEPA SIGReg configuration ( $\lambda_T = 20$ , layers  $\{0, 8\}$ ) was likewise selected from PTB-XL ablations. Neither recipe was optimized for Diag. We hypothesize that masking recipes encode domain-semantic assumptions—which temporal

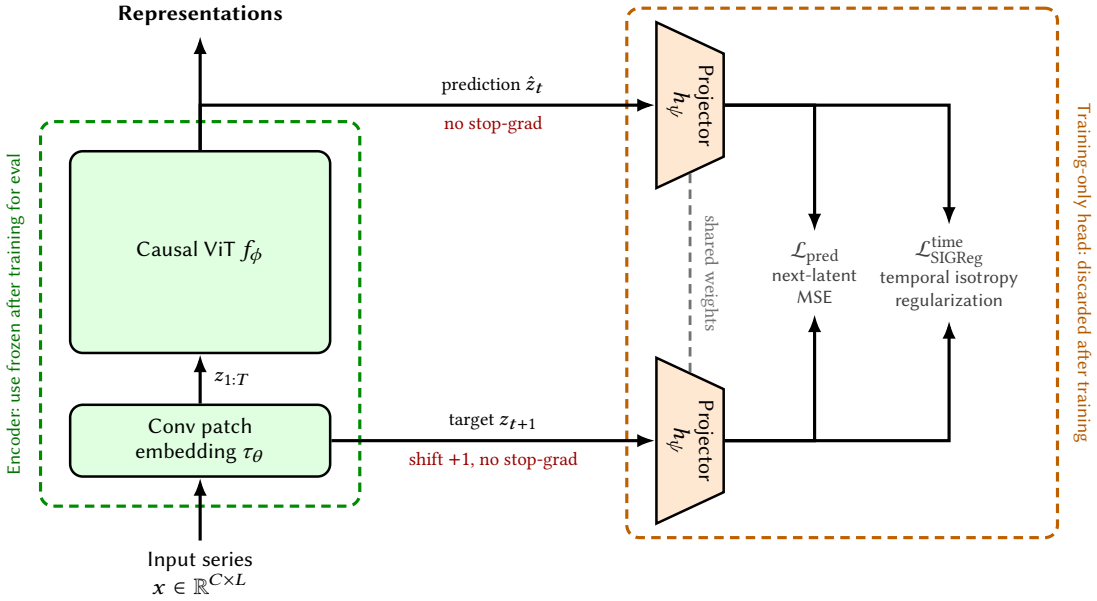


**Figure 1: LeNEPA training and what survives to evaluation.** A causal ViT autoregressively predicts the next patch embedding: the top-layer prediction  $\hat{z}_t$  and the shifted target  $z_{t+1}$  are mapped by a *shared* projector  $h_\psi$  into the space where the next-latent MSE loss  $\mathcal{L}_{\text{pred}}$  is computed, with *no stop-gradient* on the target (stabilization comes from SIGReg, not EMA/stop-gradient). Temporal SIGReg  $\mathcal{L}_{\text{SIG}}^{\text{time}}$  regularizes the projected tokens toward per-sample isotropy. The projector and losses (orange) are training-only and *discarded* at evaluation; only the encoder (green) is *kept*, and frozen probes read its best intermediate-layer representations.

regions constitute meaningful prediction targets—whereas regularization hyperparameters primarily encode optimization dynamics; moving from a masking-based view recipe to an augmentation-free regularization-based recipe should therefore reduce the domain-specific tuning required when the signal family changes. This protocol does not test the best possible Diag-tuned JEPa configuration; a JEPa recipe designed for Diag’s signal characteristics would likely recover strong performance. Rather, the experiment measures the cost of relying on ECG-masking assumptions when that recipe is reused on a structurally different signal family. **Frozen-encoder checking** asks whether one pretrained encoder can produce useful features on new downstream datasets without changing its weights. We test this by training LeNEPA-CauKer once, freezing it, extracting per-layer embeddings, and evaluating Random-Forest probes on UCR-128, following the MantisV2 testing protocol [11].

Table 2 summarizes the configuration used for the headline experiments. Table 2 and Listing 1 provide the information needed to reproduce the headline experiments.

For the NEPA/LeNEPA/JEPa comparisons on PTB-XL and Diag, all methods use the same ViT-XS backbone size and are trained for a fixed horizon of 20,000 gradient steps. For NEPA/LeNEPA, we use mean pooling over causal patch-token representations; for JEPa, we report both CLS-token and mean-pooling readouts to control for readout mismatch. Because next-embedding objectives can place the most probe-useful representation at an intermediate depth, we train offline linear probes on frozen per-layer representations for layers 0–8. For the last-step headline LeNEPA classification

**Table 1: Pretrained encoder instances used in the evaluation.** Each row is a separately pretrained checkpoint.

Encoder	Pretraining	Evaluation	Purpose
LeNEPA-PTBXL	PTB-XL	PTB-XL	In-domain ECG reference against ECG-tuned JEPa
LeNEPA-Diag	Diag	Diag	Fixed-recipe reuse across signal families
JEPa-PTBXL	PTB-XL	PTB-XL	ECG-tuned JEPa reference under the same fixed-horizon protocol
JEPa-Diag	Diag	Diag	Same ECG-tuned JEPa recipe retrained on Diag to test unchanged reuse
LeNEPA-CauKer	CauKer	UCR-128	Frozen-encoder check on external classification datasets

readouts, we use a fixed mid-layer  $L_4$  representation rather than an oracle layer; this is conservative on PTB-XL and exactly matches the best layer on Diag and the best UCR checkpoint (Table 6). For

**Table 2: Implementation and evaluation configuration for the main experiments. PTB-XL and Diag use the same fixed-horizon recipe-reuse matrix; the CauKer/UCR row documents the frozen-encoder check in Table 4.**

Item	PTB-XL / Diag fixed-horizon matrix	CauKer → UCR-128 frozen-encoder check
Training horizon and seeds	20,000 gradient steps; seeds $s \in \{0, 1, 2, 3, 4\}$ ; offline probes every 1,000 steps, including step 0	20,000 gradient steps; seed 0; UCR evaluated at each saved checkpoint and reported at the best and final checkpoints
Optimizer	AdamW, batch size 256, bfloat16; cosine learning-rate schedule $10^{-4} \rightarrow 10^{-6}$ with 1,000 warmup steps; weight decay 0.01 $\rightarrow$ 0.1; betas (0.9, 0.99)	AdamW, batch size 256, bfloat16; cosine learning-rate schedule $2 \times 10^{-4} \rightarrow 2 \times 10^{-4}$ with 1,000 warmup steps; weight decay 0.01 $\rightarrow$ 0.1; betas (0.9, 0.99)
Backbone and tokenizer	Causal ViT-XS, depth 8, 4 heads, MLP ratio 4, QK-Norm ( $\epsilon = 10^{-6}$ ), SwiGLU, RoPE; Conv1d patch embedding with $P = 25$ for length-5000 signals; $D = 192$ ; mean-pooling readout	Causal ViT-XS, depth 8, 4 heads, MLP ratio 4, QK-Norm, SwiGLU, RoPE; length-5000 CauKer sequences; $D = 256$ ; sequence-normalized scalar-statistics path added for the Mantis-facing UCR comparison
LeNEPA loss	Projected MSE next-token loss, no stop-gradient, $\lambda_{\text{pred}} = 1$ ; temporal SIGReg with $\lambda_{\text{T}} = 20$ on layers $\{0, 8\}$ ; projector is MLP+BN+ReLU with output dimension 64	Same projected next-token objective; temporal SIGReg on layers $\{0, 8\}$ with $\lambda_{\text{T}} = 2.5$ ; projector output dimension 64
JEPA view recipe	Fixed ECG-tuned masking view recipe with keep ratio $\rho \sim \text{Uniform}(0.15, 0.25)$ ; JEPA evaluated with both CLS-token and mean-pooling readouts	Not used
Probe protocol	Frozen per-layer linear probes on layers 0–8; 5,000 probe steps; AdamW, learning rate 0.01, weight decay 0, batch size 256; metrics aggregated as median and sample standard deviation across seeds	Frozen per-layer embeddings on UCR-128; Random Forest classifier with 200 trees and all 128 train/test splits; mean accuracy averaged across datasets

JEPA/NEPA baselines and dense Diag diagnostics, we retain best-layer values to avoid penalizing baselines for their different depth profiles and to keep dense probes as diagnostic rather than headline comparison metrics. We evaluate probes every 1,000 pretraining steps, including step 0, and report last-step values unless stated otherwise. For PTB-XL and Diag, each objective–dataset pair is repeated with five random seeds; tables and plots in this paper aggregate per-seed metrics as median  $\pm$  sample standard deviation. For delta summaries, we compute each seed’s difference between step 20,000 and step 0, selecting the best layer independently at each step. For early-gain summaries on AUROC/AUPRC, define the normalized gain

$$r_m(t) = \frac{m(t) - m(0)}{m(20,000) - m(0)} \quad (4)$$

for metric  $m$  at pretraining step  $t$ , and let  $\tau_q(m)$  be the first offline-probe evaluation step at which  $r_m(t) \geq q$ . We compute these thresholds on the median learning curves in Figure 2; because probes are evaluated every 1,000 steps,  $\tau_q$  is a discrete step count rather than an interpolated time.

PTB-XL is a 12-lead ECG classification dataset with clinically meaningful multi-label targets [20]. This benchmark is a useful in-domain test because ECG\_JEPA is a strong baseline designed around ECG-specific JEPA augmentations [21]. To test fixed-recipe reuse across a different signal family, we construct **Diag**, a synthetic diagnostic corpus generated with the Aionoscope library [6], implemented as an online generator rather than a fixed finite dataset. Aionoscope provides a Process-to-View generator that renders latent process states into observed time series and emits exact categorical and dense labels from the same state. Our Diag stream uses Aionoscope’s Primitive Process Mixtures generator, but it is a LeNEPA evaluation stream rather than the public Aionoscope benchmark sweep: here we use length-5000 univariate sequences, exactly 2 active components per sample, and a custom imbalanced component sampler. Each sample is generated by selecting active latent components from a fixed inventory of 14 component types spanning constant baselines, noise processes, trends, periodic waveforms, and sparse events. The main stream is intentionally imbalanced: most components have sampling weight 1.0, while six rare components have weight 0.02 (gaussian\_noise, log\_trend, square, spike, level\_change, and gaussian).

Diag exposes two kinds of targets used for frozen-backbone probing. Categorical targets are multi-hot indicators of the active component types and are evaluated with macro AUROC/AUPRC. Dense targets are scalar generative parameters recorded by the generator metadata, including noise scale, trend coefficients, periodic amplitude/frequency/phase/offset, and event time/amplitude/width; disabled components are masked for the corresponding dense target. SSL training never uses these targets. Pretraining and probing streams use separate fixed RNG streams, so probes evaluate fresh generated samples from the same distribution rather than memorized training examples.

Finally, we include a frozen-encoder check by testing LeNEPA-CauKer trained on CauKer [23] on the full UCR archive of 128 univariate classification datasets [8]. Unlike the PTB-XL/Diag fixed-recipe study, the CauKer-to-UCR experiment evaluates a single frozen LeNEPA checkpoint across 128 external datasets. For this experiment, we follow the Mantis frozen-feature protocol: extract frozen per-layer sequence embeddings, train a Random Forest classifier on each dataset’s training split, evaluate on its test split, and average accuracy across datasets [11, 23]. We use the original Mantis Random-Forest result as the primary published anchor, and report NuTime and MOMENT only as protocol-matched context from the MantisV2 Random-Forest comparison [12, 16].

## 4 Experiments

We evaluate frozen-backbone representations using per-layer probes. For time series, we evaluate fixed-recipe reuse on PTB-XL (12-lead ECG classification) and Diag (classification + dense regression), then use UCR-128 as a separate frozen-encoder check.

*Fixed-recipe reuse: PTB-XL vs. Diag.* The baseline JEPA model [21] is tuned for ECG and relies on dataset-specific augmentations, and thus performs well on the dataset it was designed for. In this in-domain regime, LeNEPA remains competitive, showing that eliminating augmentations does not preclude useful frozen features. We then test fixed-recipe reuse by training both LeNEPA and JEPA again on Diag while keeping each method’s recipe unchanged. As shown by Figure 2, the JEPA configuration that is strong on PTB-XL is weaker when reused unchanged on Diag; JEPA-Diag’s training gains shrink markedly, whereas LeNEPA-Diag retains strong training gains and beats JEPA-Diag both in final performance and training dynamics. This does not rule out a Diag-tuned JEPA recipe; a

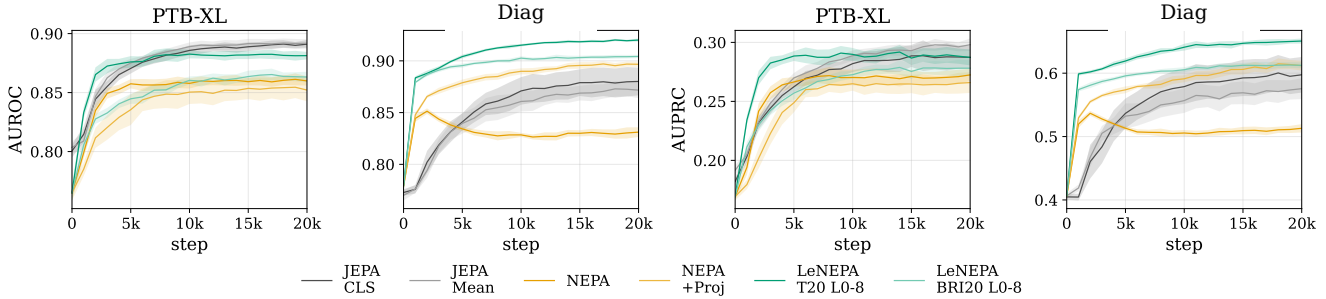


**Figure 2: PTB-XL/Diag fixed-recipe reuse experiment: best-layer frozen-backbone classification dynamics over the fixed 20,000-step pretraining horizon. Curves show AUROC/AUPRC at each offline-probe evaluation step for PTB-XL and Diag. This tests recipe portability, not shared-checkpoint transfer or a claim that Diag-tuned JEPAs cannot work. Both methods are trained separately on each dataset; the fixed ECG-tuned JEPAs recipe remains strong in-domain but is weaker when reused unchanged on Diag.**

**Table 3: PTB-XL/Diag fixed-horizon experiment matrix at the last step (20,000 updates) for the controlled five-seed comparisons. JEPAs/NEPAs rows report best-layer frozen-backbone probes; LeNEPA classification columns use a fixed  $L_4$  readout, while LeNEPA dense Diag columns report metric-specific best-layer diagnostic probes. Values are aggregated across seeds as median(std), with std shown in  $10^{-3}$  units.**

model	config	PTB-XL		Diag					
		AUROC $\uparrow$	AUPRC $\uparrow$	AUROC $\uparrow$	AUPRC $\uparrow$	MSE $\downarrow$	MAE $\downarrow$	Pearson $\uparrow$	$R^2$ $\uparrow$
JEPAs	CLS	<b>0.891(3)</b>	0.287(9)	0.880(13)	0.597(28)	1.065(13)	0.515(5)	0.480(12)	-0.005(24)
JEPAs	Mean	<b>0.892(3)</b>	<b>0.298(5)</b>	0.872(7)	0.576(16)	1.113(13)	0.548(5)	0.462(11)	-0.514(291)
NEPAs		0.860(3)	0.272(5)	0.831(4)	0.513(6)	1.001(9)	0.461(3)	0.522(4)	0.197(24)
NEPAs	+Proj	0.852(9)	0.266(8)	<u>0.897(2)</u>	<u>0.612(7)</u>	<u>0.827(8)</u>	<b>0.382(3)</b>	<b>0.610(7)</b>	<b>0.348(23)</b>
LeNEPAs	T20 L0-8	<u>0.880(6)</u>	<u>0.285(5)</u>	<b>0.920(1)</b>	<b>0.650(4)</b>	<b>0.797(12)</b>	<u>0.405(4)</u>	<u>0.584(6)</u>	0.164(105)

**Table 4: UCR-128 frozen-encoder check. We report mean accuracy over all 128 UCR datasets using frozen sequence embeddings and a Random Forest classifier. The table lists each model’s pretraining data because baselines differ in architecture, objective, and whether UCR/UEA training data or larger heterogeneous corpora were used. The LeNEPA-CauKer row reports the best checkpoint over the fixed 20,000-step trajectory; Mantis is the closest published CauKer-only Mantis-family anchor, and NuTime/MOMENT provide protocol-matched context from the same Random-Forest comparison.**

Model	Pretrain data	Params	Attention	Tokenizer / input engineering	SSL objective	Acc. (%)
LeNEPA	CauKer; no UCR	6.3M	causal	Conv patches + global stats	latent prediction; no aug.	77.65
Mantis	CauKer; no UCR	8.1M	bidirectional	Conv patches + patch stats + diff	contrastive; crop aug.	78.81
NuTime [16]	incl. UCR/UEA train	2.0M	bidirectional	Window shape + window stats	BYOL; crop aug.	77.32
MOMENT [12]	incl. UCR/UEA train	161M	bidirectional	T5 patches	masked reconstruction	77.89

LeNEPA-CauKer peaks at 77.65% at 17,000 steps and remains at 77.20% at the final 20,000-step checkpoint (Figure 3). LeNEPA-CauKer row adds MSSE for this Mantis-facing UCR comparison because Mantis itself uses an MSSE-encoded scalar-statistics path; the main LeNEPA experiments elsewhere in the paper do not rely on MSSE. NuTime/MOMENT entries use the Random-Forest UCR-128 averages reported in MantisV2 [11].

JEPAs recipe designed for Diag’s signal characteristics would likely recover competitive performance. Rather, the experiment identifies *ECG-masking assumptions*—the semantic tie between JEPAs’s view recipe and ECG morphology—as a source of fragility when that recipe is reused on a structurally different signal family. A general-purpose JEPAs masking recipe might transfer better, but would still require per-domain view engineering: exactly the cost that a no-augmentation objective avoids by design. Finally, Figure 2

summarizes early learning dynamics under the time-to-gain definition in Section 3. On the median AUROC/AUPRC curves, LeNEPA reaches 80% of its final gain after 2–5k updates across PTB-XL and Diag, whereas the faster JEPAs readout reaches the same threshold after 5–10k updates; because probes are evaluated every 1,000 steps these thresholds are coarse discrete counts and per-seed timing varies. The 90% threshold is less uniform—LeNEPA reaches it after 5–10k updates, while JEPAs typically reaches it after 10–15k updates—so we interpret these observations as qualitative evidence

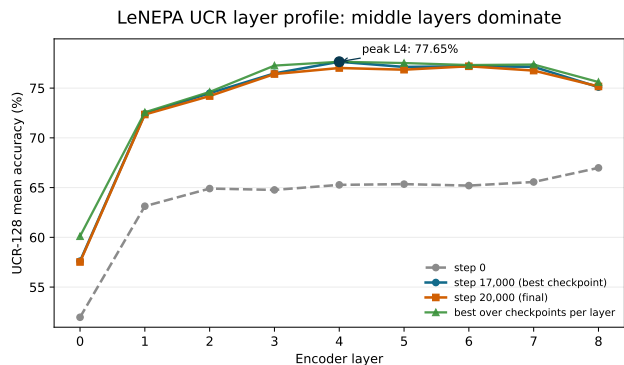


**Figure 3: UCR-128 layer-profile diagnostic for the LeNEPA-CauKer run used in Table 4. Each point is mean Random-Forest accuracy over the 128 UCR datasets for one frozen backbone layer. Intermediate layers outperform the final layer: the run peaks at 77.65% at 17,000 steps ( $L_4$ ) and remains at 77.20% at the final 20,000-step checkpoint ( $L_6$ ).**

of faster early representation acquisition in this fixed-recipe protocol.

*Frozen-encoder check: CauKer to UCR-128.* We use UCR-128 as a frozen-encoder check that complements the fixed-recipe reuse study. We choose Mantis as the primary comparator because it is a state-of-the-art SSL/foundation architecture for time-series classification and is close to LeNEPA in the relevant evaluation regime: a frozen time-series encoder followed by a lightweight classifier [10, 11]. UCR-128 classification accuracy is Mantis’s headline contribution; its architecture was purpose-built for this setting: bidirectional attention (full sequence context), a handcrafted first-difference branch, and a contrastive objective with Random Crop Resize augmentations. The closest published anchor from this architecture uses frozen Mantis representations and reports 78.81% average accuracy on all 128 UCR datasets with a Random Forest classifier. As shown in Table 4, our LeNEPA-CauKer run peaks at 77.65% over the fixed 20k-step pretraining trajectory (single seed) and remains at 77.20% at the final checkpoint (Figure 3). We treat this single-seed result as an existence proof: a LeNEPA encoder with causal attention, no augmentations, and no first-difference branch—each a structural disadvantage relative to Mantis for UCR classification—can already produce frozen features competitive with a model that was specifically designed and optimised for this benchmark. Additional seeds would characterise variance; this run establishes that the no-augmentation causal recipe can reach the Mantis neighbourhood without any UCR-specific engineering. NuTime and MOMENT in the same MantisV2 Random-Forest UCR table are reported as 77.32% and 77.89%, respectively; the best LeNEPA checkpoint is above NuTime and within 0.24 percentage points of MOMENT [12, 16]. Because this comparison uses a single LeNEPA pretraining seed, a best checkpoint over the trajectory, and baselines with different pretraining corpora and architectures, we treat it as protocol-matched context for the frozen features. We therefore do not treat stronger MantisV2 final-comparison or leaderboard

numbers as direct baselines, because they are designed for leaderboard performance through heavier model and test-time/evaluation choices rather than for isolating the effect of a no-augmentation objective.

The following diagnostics summarize the main ablations needed to interpret the results.

## 5 Ablations and Diagnostics

Diag acts as diagnostic instrumentation rather than as a paper contribution. Each generated sequence has known latent factors and categorical/dense targets; SSL pretraining does not use these labels, and they are used only after freezing the backbone to probe which factors are linearly recoverable from each layer.

Table 5 summarizes the controlled ablations behind the main LeNEPA design choices. Because the page limit prevents full ablation tables, we report the design-level conclusions here. The projector rows test the Guillotine Regularization idea that SSL losses can be applied in a disposable head while evaluating the truncated backbone [4]. As Table 3 shows, NEPA with a projector (NEPA + Proj) is already a strong baseline: it outperforms LeNEPA on several dense Diag metrics (MAE, Pearson,  $R^2$ ) while LeNEPA leads on classification (AUROC, AUPRC) and MSE. The contribution of temporal SIGReg over NEPA + Proj is therefore most clearly visible on classification and training dynamics, while the dense regression picture is more mixed.

Finally, layer-wise probing reveals a pattern that is increasingly important for latent-prediction encoders. Across both datasets, JEPA probe performance tends to improve with depth and peak near the top layers. In contrast, NEPA and LeNEPA often achieve their best probe scores at intermediate layers (frequently around  $l \approx 3-5$ ), with the final layer sometimes underperforming these mid-level representations. This suggests that the deepest blocks of next-embedding predictors can partially specialize to the prediction task, while intermediate layers retain more probe-useful features.

*Layer-selection sensitivity.* The best-layer protocol is an oracle upper bound. The key question is therefore whether this oracle choice materially changes the conclusions. We check this by comparing oracle selection to a fixed mid-layer readout. Table 6 compares the oracle best layer with a fixed  $L_4$  readout and the final transformer layer  $L_8$  for LeNEPA classification results. The classification optima are concentrated in the middle of the backbone: PTB-XL peaks at  $L_5$ , while Diag and the best UCR checkpoint peak at  $L_4$ . Across the five-seed PTB-XL and five-seed Diag classification evaluations, using the fixed  $L_4$  readout removes almost all of the oracle advantage, whereas using the final layer can be substantially worse. Thus, the LeNEPA classification conclusions do not rely on per-dataset layer tuning; dense Diag probes are more metric-dependent and should be read primarily as diagnostics of where information appears in the backbone.

## 6 Limitations and Future Work

While LeNEPA removes one source of time-series SSL engineering by avoiding augmentations, our current study tests recipe portability rather than claiming a foundation encoder. The convolutional tokenizer still depends on dataset-specific design choices such as kernel size and stride, implicitly assumes regular sampling, and

**Table 5: Compact ablation summary supporting the LeNEPA design choices.**

Design question	Controlled ablation	Main observation	Implication
Projector loss space	Guillotine-style projector: NEPA/LeNEPA trained with and without the projector	Projector-enabled variants improve 22/24 last-step probe comparisons.	Compute prediction and SIGReg losses in projected space, then discard the projector for evaluation.
Projector capacity	Output width, hidden width, and MLP depth of the Guillotine-style projector	Larger or deeper projectors do not improve performance over the fixed projector used in the main runs.	The main projector effect comes from separating the loss space from the evaluated backbone space, not from adding projector capacity.
SIGReg axis	Temporal (T) SIGReg versus batch-wise (B), pooled-representation (R), innovation/difference (I), and batch-time (BT) placements	Temporal SIGReg is the only single-component placement with sustained frozen-backbone gains across PTB-XL and Diag.	Use Temporal SIGReg as the LeNEPA anti-collapse stabilizer.
SIGReg layer placement	Temporal SIGReg on both prediction/target sides $\{0, 8\}$ vs. one side or inner layers	Regularizing both sides of the prediction relation is more stable in our fixed-recipe runs; target-only or off-path regularization can degrade or collapse.	Apply SIGReg where it directly counterbalances the next-embedding prediction loss.
JEPA view recipe	PTB-XL JEPA keep-ratio $(0.15, 0.25)$ vs. $(0.05, 0.10)$ and $(0.30, 0.40)$	A 2-3 $\times$ change in masking strength substantially degrades probe dynamics.	Augmentation/view hyperparameters can be sensitive, motivating a no-augmentation objective.

**Table 6: Layer-selection sensitivity motivating the fixed-L4 LeNEPA classification readout. Best-layer values are oracle selections over probed layers; fixed L4 uses one mid-layer readout across datasets; L8 is the final transformer layer. Parentheses report the difference from the oracle value.**

Dataset	Metric	Oracle layer	Oracle	Fixed L4 ( $\Delta$ )	Final L8 ( $\Delta$ )
PTB-XL	AUROC	L5	0.880	0.880 (0.000)	0.835 (-0.045)
PTB-XL	AUPRC	L5	0.287	0.285 (-0.002)	0.203 (-0.084)
Diag	AUROC	L4	0.920	0.920 (0.000)	0.895 (-0.025)
Diag	AUPRC	L4	0.650	0.650 (0.000)	0.607 (-0.043)
UCR-128	Accuracy	L4	77.65	77.65 (0.00)	75.10 (-2.55)

may limit transfer across signals with different temporal scales. Although the PTB-XL/Diag fixed-recipe runs use the same temporal SIGReg setting, SIGReg still introduces scale and placement hyperparameters; the CauKer/UCR run uses a smaller temporal scale in a different tokenizer configuration, so principled defaults across dataset scales and tokenizers remain future work. Diag is also a synthetic corpus generated with Aionoscope [6], so conclusions drawn from it should be read as controlled state-accessibility evidence rather than as direct evidence of real-world diagnostic transfer. Some diagnostic analyses and baseline comparisons still report best-layer values; those should be treated as oracle upper bounds unless a layer is fixed a priori or selected using labeled validation data. For LeNEPA classification, the reported last-step readout is fixed to L4 and is stable relative to the oracle choice (Table 6). The UCR-128 frozen-encoder check broadens the evidence beyond PTB-XL and Diag, but it is still univariate and uses one pre-training seed; broader UEA-style multivariate evaluations remain necessary.

## 7 Conclusion

Time-series SSL recipes are often entangled with view and augmentation choices that may be safe in one signal family but mismatched in another. We studied this issue as a *fixed-recipe stress test*: keep each method’s SSL recipe unchanged, retrain on a new pretraining distribution, and evaluate whether frozen representations remain useful. This setting is intentionally narrower than fully tuned benchmark comparison; it measures the cost of recipe reuse, not the best attainable performance after retuning.

We proposed **LeNEPA**, a no-augmentation next-embedding prediction architecture that replaces EMA/stop-gradient stabilization with temporal SIGReg and applies the predictive loss in a disposable projected space. Under the PTB-XL/Diag fixed-horizon protocol, an ECG-tuned JEPA recipe remains strong in-domain but weakens when reused unchanged on Diag, while LeNEPA preserves useful frozen-probe gains under the same unchanged-recipe rule. The learning curves also suggest faster early representation acquisition for LeNEPA in this protocol, though the evidence should be read as a fixed-recipe result rather than a claim about optimally tuned JEPA.

As a separate frozen-encoder check, a CauKer-pretrained LeNEPA checkpoint falls in the range of protocol-matched UCR-128 Random-Forest anchors while avoiding handcrafted augmentations and using a causal backbone. This check provides external context for the learned features, but it is not a definitive foundation-model or leaderboard claim: it uses one pretraining seed, a best checkpoint over the trajectory, and a UCR-specific comparison setup.

We thus conclude that augmentation-free latent prediction is a promising building block for time-series representation learning

when the operational constraint is to reuse an SSL recipe with minimal per-dataset view engineering.

## References

- [1] Mahmoud Assran, Quentin Duval, Ishan Misra, Piotr Bojanowski, Pascal Vincent, Michael Rabbat, Yann LeCun, and Nicolas Ballas. 2023. Self-Supervised Learning from Images with a Joint-Embedding Predictive Architecture. <https://arxiv.org/abs/2301.08243> arXiv:2301.08243.
- [2] Randall Balestriero and Yann LeCun. 2025. LeJPA: Provable and Scalable Self-Supervised Learning Without the Heuristics. <https://arxiv.org/abs/2511.08544> arXiv:2511.08544.
- [3] Adrien Bardes, Quentin Garrido, Jean Ponce, Xinlei Chen, Michael Rabbat, Yann LeCun, Mahmoud Assran, and Nicolas Ballas. 2024. Revisiting Feature Prediction for Learning Visual Representations from Video. <https://arxiv.org/abs/2404.08471> arXiv:2404.08471.
- [4] Florian Bordes, Randall Balestriero, Quentin Garrido, Adrien Bardes, and Pascal Vincent. 2022. Guillotine Regularization: Why removing layers is needed to improve generalization in Self-Supervised Learning. <https://arxiv.org/abs/2206.13378> arXiv:2206.13378.
- [5] Mathilde Caron, Hugo Touvron, Ishan Misra, Hervé Jégou, Julien Mairal, Piotr Bojanowski, and Armand Joulin. 2021. Emerging Properties in Self-Supervised Vision Transformers. <https://arxiv.org/abs/2104.14294> arXiv:2104.14294.
- [6] Alexander Chemeris, Ming Jin, and Randall Balestriero. 2026. Aionoscope: Debugging Latent-State Accessibility in Time-Series Representations. In *The 12th Mining and Learning from Time Series Workshop (MiLeTS '26), held in conjunction with KDD 2026*. <https://github.com/langotime/aionoscope>
- [7] Ting Chen, Simon Kornblith, Mohammad Norouzi, and Geoffrey Hinton. 2020. A Simple Framework for Contrastive Learning of Visual Representations. <https://arxiv.org/abs/2002.05709> arXiv:2002.05709.
- [8] Hoang Anh Dau, Anthony Bagnall, Kaveh Kamgar, Chin-Chia Michael Yeh, Yan Zhu, Shaghayegh Gharghabi, Chotirat Ann Ratanamahatana, and Eamonn Keogh. 2019. The UCR time series archive. *IEEE/CAA Journal of Automatica Sinica* 6, 6 (2019), 1293–1305.
- [9] Emadeldeen Eldele, Mohamed Ragab, Zhenghua Chen, Min Wu, Chee Keong Kwoh, Xiaoli Li, and Cuntai Guan. 2021. Time-Series Representation Learning via Temporal and Contextual Contrasting. <https://arxiv.org/abs/2106.14112> arXiv:2106.14112.
- [10] Vasilii Feofanov, Songkang Wen, Marius Alonso, Romain Ilbert, Hongbo Guo, Malik Tiomoko, Lujia Pan, Jianfeng Zhang, and Ievgen Redko. 2025. Mantis: Light-weight calibrated foundation model for user-friendly time series classification. *arXiv preprint arXiv:2502.15637* (2025).
- [11] Vasilii Feofanov, Songkang Wen, Jianfeng Zhang, Lujia Pan, and Ievgen Redko. 2026. MantisV2: Closing the Zero-Shot Gap in Time Series Classification with Synthetic Data and Test-Time Strategies. doi:10.48550/arXiv.2602.17868 arXiv:2602.17868; ICLR 2026 TSALM Workshop Poster.
- [12] Mononito Goswami, Konrad Szafer, Arjun Choudhry, Yifu Cai, Shuo Li, and Artur Dubrawski. 2024. MOMENT: A family of open time-series foundation models. *arXiv preprint arXiv:2402.03885* (2024).
- [13] Jean-Bastien Grill, Florian Strub, Florent Altché, Corentin Tallec, Pierre H. Richemond, Elena Buchatskaya, Carl Doersch, Bernardo Avila Pires, Zhaohan Daniel Guo, Mohammad Gheshlaghi Azar, Bilal Piot, Koray Kavukcuoglu, Rémi Munos, and Michal Valko. 2020. Bootstrap your own latent: A new approach to self-supervised Learning. <https://arxiv.org/abs/2006.07733> arXiv:2006.07733.
- [14] Kaiming He, Xinlei Chen, Saining Xie, Yanghao Li, Piotr Dollár, and Ross Girshick. 2021. Masked Autoencoders Are Scalable Vision Learners. <https://arxiv.org/abs/2111.06377> arXiv:2111.06377.
- [15] Kaiming He, Haoqi Fan, Yuxin Wu, Saining Xie, and Ross Girshick. 2020. Momentum Contrast for Unsupervised Visual Representation Learning. <https://arxiv.org/abs/1911.05722> arXiv:1911.05722.
- [16] Chenguo Lin, Xumeng Wen, Wei Cao, Congrui Huang, Jiang Bian, Stephen Lin, and Zhirong Wu. 2024. NuTime: Numerically Multi-Scaled Embedding for Large-Scale Time-Series Pretraining. *Transactions on Machine Learning Research* (2024). <https://openreview.net/forum?id=TwSBZ0p9u>
- [17] Ziyu Liu, Azadeh Alavi, Minyi Li, and Xiang Zhang. 2024. Guidelines for Augmentation Selection in Contrastive Learning for Time Series Classification. <https://arxiv.org/abs/2407.09336> arXiv:2407.09336.
- [18] Sana Tonekaboni, Danny Eytan, and Anna Goldenberg. 2021. Unsupervised Representation Learning for Time Series with Temporal Neighborhood Coding. <https://arxiv.org/abs/2106.00750> arXiv:2106.00750.
- [19] Ashish Vaswani, Noam Shazeer, Niki Parmar, Jakob Uszkoreit, Llion Jones, Aidan N. Gomez, Lukasz Kaiser, and Illia Polosukhin. 2017. Attention Is All You Need. <https://arxiv.org/abs/1706.03762> arXiv:1706.03762.
- [20] Patrick Wagner, Nils Strodthoff, Ralf-Dieter Boussejot, Dieter Kreiseler, Fatima I. Lunze, Wojciech Samek, and Tobias Schaeffter. 2020. PTB-XL, a large publicly available electrocardiography dataset. *Scientific Data* 7, 1 (2020), 154. doi:10.1038/s41597-020-0495-6
- [21] Kuba Weimann and Tim O. F. Conrad. 2024. Self-Supervised Pre-Training with Joint-Embedding Predictive Architecture Boosts ECG Classification Performance. <https://arxiv.org/abs/2410.13867> arXiv:2410.13867.
- [22] Gerald Woo, Chenghao Liu, Doyen Sahoo, Akshat Kumar, and Steven Hoi. 2022. CoST: Contrastive Learning of Disentangled Seasonal-Trend Representations for Time Series Forecasting. <https://arxiv.org/abs/2202.01575> arXiv:2202.01575.
- [23] Shifeng Xie, Vasilii Feofanov, Marius Alonso, Ambroise Odonnat, Jianfeng Zhang, Themis Palpanas, and Ievgen Redko. 2025. CauKer: classification time series foundation models can be pretrained on synthetic data only. *arXiv preprint arXiv:2508.02879* (2025).
- [24] Sihan Xu, Ziqiao Ma, Wenhao Chai, Xuweiyi Chen, Weiyang Jin, Joyce Chai, Saining Xie, and Stella X. Yu. 2025. Next-Embedding Prediction Makes Strong Vision Learners. <https://arxiv.org/abs/2512.16922> arXiv:2512.16922.
- [25] Zhihan Yue, Yujing Wang, Juanyong Duan, Tianmeng Yang, Congrui Huang, Yunhai Tong, and Bixiong Xu. 2022. TS2Vec: Towards Universal Representation of Time Series. <https://arxiv.org/abs/2106.10466> arXiv:2106.10466.

